Assessment of the Direct Economic Losses of Flood Disasters Based on the Spatial Valuation of Land Use and Quantification of Vulnerabilities: A Case Study of the 2014 Flood in Lishui city, China

Haixia Zhang[1, 2], Weihua Fang[1, 2, 3], Hua Zhang[1, 2]

[1] Key Laboratory of Environmental Change and Natural Disaster of Ministry of Education, Faculty of Geographical Science, Beijing Normal University, Beijing 100875, China
[2] Academy of Disaster Risk Science, Faculty of Geographical Science, Beijing Normal University, Beijing 100875, China
[3] Southern Marine Science and Engineering Guangdong Laboratory, Guangzhou 511458, China

Correspondence: Weihua Fang (weihua.fang@bnu.edu.cn)

Abstract. The refined assessment of the direct economic losses of flood disasters is important for emergency dispatch and risk management in small- and medium-sized cities. ~~There are still great challenges in the accuracy and timeliness of the previous research methods.~~ In this study, a single flood disaster in Lishui city in 2014 was taken as an example to study and verify a method for the rapid and refined assessment of direct economic loss. First, based on a field investigation, the inundation ~~range and submerged depth~~ data simulated by the ~~flooding~~one-dimensional hydrodynamic model and geographic information system (GIS) analysis method were verified. Next, the urban land use status map and high-~~precision~~resolution land use classifications based on remote sensing ~~classification~~ data were fused and combined with expert questionnaire surveys, thereby providing the 47 types and values of ~~disaster-bearing bodies.~~land use. Then, based on the ~~existing~~ previous depth-damage function, the vulnerability ~~curve database was summarized, and the~~ curves of 47 types of land use in Liandu district were ~~calibrated~~fitted by the lognormal cumulative distribution function and optimized using disaster loss ~~reporting~~report data. Finally, the ~~spatial~~ distributions of the ~~flood disaster~~ loss ratio and loss value were estimated by spatial analysis. It is found that the constructed land use ~~map~~data has detailed types and value attributes as well as high ~~precision spatial information~~ resolution. Secondly, the vulnerability curves after function fitting and calibration effectively reflect the change characteristics of land use loss ratio in this area. Finally, except for the 3 types of land for agriculture, recreational and sports facilities, and parks green spaces, the optimized simulated total loss is 322.6 million yuan, which is 0.16% higher than the statistics report data. The estimated loss ratio and loss value ~~distributions~~ can accurately reflect the ~~spatial~~distribution pattern of ~~flood~~ disaster ~~loss~~losses, which is useful for the government to formulate effective disaster reduction and relief measures.

Key words: Flood disaster, Direct economic loss, Loss assessment, Vulnerability curve

1 Introduction

Refined assessments of the direct economic losses of flood disasters are very important in disaster emergency rescue and urban flood risk management (Li et al., 2017; UNISDR, 2015). The results of a rapid quantitative assessment of disaster losses with

high spatial resolution not only provide suggestions for the government to formulate emergency dispatch management measures, such as releasing disaster information, deploying rescue forces and relief materials, and the emergency resettlement of disaster victims, but also lay a data foundation for decision-makers to plan sponge cities and formulate flood risk management systems and climate change adaptation policies (Alfieri et al., 2016; Merz et al., 2010). Among them, sponge city refers to a city that can be as flexible as a sponge in adapting to environmental changes and natural disasters. It absorbs, stores, infiltrates and purifies water when it rains, and releases and reuses the stored water when necessary (Yu et al., 2015). In order to solve the problems of water shortage, waterlogging and water pollution caused by rapid urbanization, the Chinese government launched the sponge city construction plan on December 31, 2014 (MHURD, 2014), which can effectively alleviate urban waterlogging, reduce runoff pollution, save water resources and improve ecological environment.

As a key component of flood risk assessment, flood loss assessment has been extensively analyzed by researchers (Falter et al., 2015; Koks et al., 2015). The flood loss data obtained from a comprehensive high-quality field survey after a disaster can accurately reflect the disaster loss situation and has important reference value for the establishment and verification of flood loss models (Carisi et al., 2018). However, given that loss data can only be obtained after a flood, these data cannot provide timely guidance for disaster relief. In addition, the collection of the ~~Collecting~~ loss data is also time-consuming and laborious~~, which supports the further development of flood loss assessment models~~.

Due to the development of existing flood loss assessment models, there are relatively mature methods and tools (EMA, 2002; Scawthorn et al., 2006), and the popularization of flood insurance provides relatively complete socioeconomic and disaster loss data, thus, disaster losses can be quickly assessed when floods occur (Hsu et al., 2011). The United States (~~Smith D, 1994~~ Custer and Nishijima, 2015; USACE, 2006), the United Kingdom (Stephenson and D'Ayala, 2013), Japan (Dutta et al., 2003), Canada (NRC, 2017), Australia (Hasanzadeh Nafari et al., 2016b, 2016a; Wehner et al., 2017), Italy (Amadio et al., 2016), China (Li et al., 2012; Penning-Rowsell et al., 2013), and other flood-prone countries have carried out a large number of loss assessment studies using different classification systems of exposure data~~disaster-bearing bodies~~ and then used the existing loss database and post-disaster investigation data to establish local flood vulnerability functions.

In addition, with the development and application of ~~hydrological models and hydrodynamic models,~~ geographic information systems (GISs), remote sensing (RS), hydrological models, and hydrodynamic models (Elkhrachy, 2015; Jonkman et al., 2008), flood loss assessment models based on depth-damage functions have been improved (Komolafe et al., 2018). However, there are still some problems. First, there is a lack of a depth-damage functions for use in specific areas, which need to be constructed through extensive post-disaster survey data (Albano et al., 2018). Second, the effect and accuracy of the assessment are affected by the scale of the exposure data ~~disaster-bearing body~~. The microscale loss assessment model for each affected object (building, infrastructure object, etc.) has poor applicability. However, mesoscale exposure~~disaster-bearing body~~ data mainly refer to land use obtained through remote sensing (RS) interpretation (Merz et al., 2010). Although mesoscale data can effectively be used to extract the spatial distribution of buildings, it is difficult to identify the occupancy types of buildings. These problems lead to high uncertainties and disparities in flood loss assessments (Gerl et al., 2016; Pinelli et al., 2020).

With the introduction of fuzzy mathematics, gray system models, genetic algorithms, and other mathematical methods, the rapid estimation and prediction of regional flood direct economic loss can be realized (Qie and Rong, 2017; Zhao et al., 2014; Zhou et al., 2006), which can effectively reflect the overall situation of economic losses in a large region and reduce the investment in human and material resources. However, due to the lack of high-resolution ~~spatial~~ location information, this approach cannot provide timely and effective suggestions for the government to formulate targeted emergency scheduling plans.

To effectively improve the accuracy, timeliness, and practicability of flood disaster loss assessment, a refined assessment model of single-flood disaster losses in small- and medium-sized cities ~~is~~was explored in this paper. The heavy rainfall from 18 August 2014 to 20 August 2014 caused ~~serious~~severe river backflow and urban waterlogging, and many houses and roads were flooded in Lishui city. Therefore, taking this flood disaster as an example, a refined assessment model for the direct economic losses of regional flooding disasters was constructed. The model ~~includes~~included flood inundation ~~models, the spatial distribution of~~simulation, land use ~~types, the~~ type fusion, land use value quantification ~~of land use values~~, vulnerability ~~curve~~function fitting~~,~~ and optimization, as well as loss ratio and loss value ~~estimations~~estimation.

2 Materials

2.1 Study area

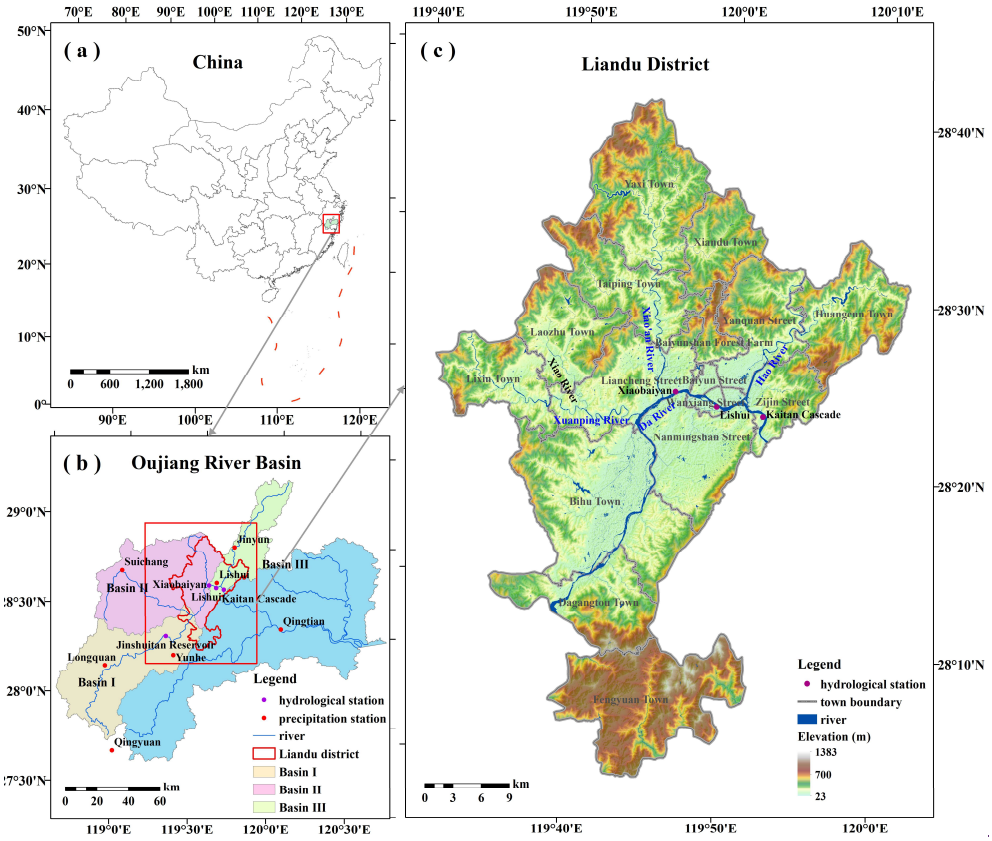
(a)
China
km
0 600 1,200 1,800
(b)
Oujiang River Basin
Jinyun
Suichang
Lishui
Basin III
Basin II
Xiaobaiyan
Lishui-Kaitan Cascade
Qingtian
Jinshuitan Reservoir
Yunhe
Longquan
Basin I
Qingyuan
Legend
hydrological station
precipitation station
river
Liandu district
Basin I
Basin II
Basin III
km
0 20 40 60
(c)
Liandu District
Yaxi Town
Xiaodu Town
Taiping Town
Laozhu Town
Tanquan Street
Huangcaoyu Town
Baiyunshan Forest Farm
Lixin Town
Liancheng Street
Baiyun Street
Xiaobaiyan
Wanxiang Street
Zijin Street
Lishui
Kaitan Cascade
Nanmingshan Street
Bihu Town
Dagangtou Town
Fengyuan Town
Xiao Ji River
Hua River
Xiao River
Xuanping River
Da River
Legend
hydrological station
town boundary
river
Elevation (m)
1383
700
23
km
0 3 6 9
70°E 80°E 90°E 100°E 110°E 120°E 130°E
50°N 40°N 30°N 20°N 10°N 0°
90°E 100°E 110°E 120°E
29°0'N 28°30'N 28°0'N 27°30'N
119°0'E 119°30'E 120°0'E 120°30'E
119°40'E 119°50'E 120°0'E 120°10'E
28°40'N 28°30'N 28°20'N 28°10'N
119°40'E 119°50'E 120°0'E

80

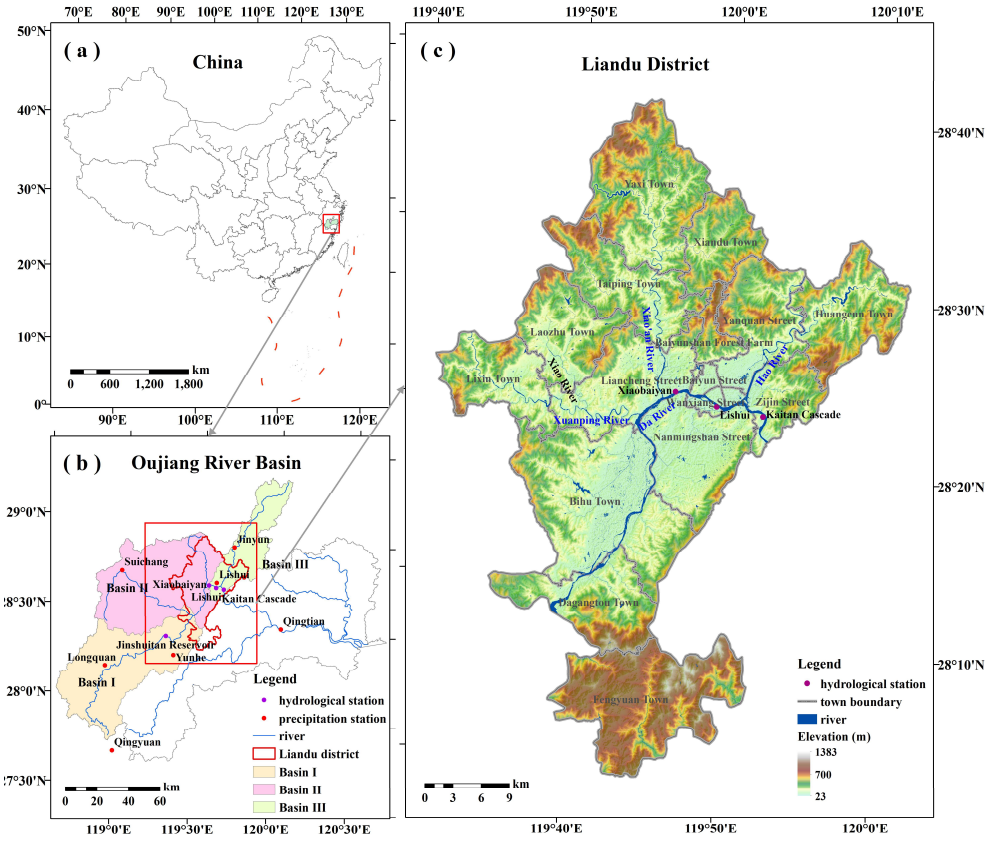

Figure 1. Location of the study area. (a. The location of Oujiang River Basin in China. b. The distribution of hydrological stations, precipitation stations, rivers and sub basins in Oujiang River Basin, and the location of Liandu ~~District~~district in Oujiang River Basin. c. The terrain distribution and town boundary of Liandu district.)

Liandu ~~District~~district is in southwestern Zhejiang Province, between 28°06′ N-28°44′ N and 119°32′ E-120°08′ E (Figure 1). This district is in the middle reaches of the Oujiang River Basin, surrounded ~~by hills and~~ mountains ~~with plains~~and a plain in the middle, ~~spanning~~with a total area of approximately 1,502 km^2. Liandu ~~District is situated within~~is a district under the jurisdiction of Lishui city, with a relatively concentrated population and socioeconomic status. As a result of both urban planning and topography, the flood disaster in Liandu ~~District caused~~district causes heavy losses. Because topography has a great impact on hydrology and hydrodynamics, it is easy to ignore regional differences based on administrative units. Considering the impact of the Jinshuitan Reservoir operation, the upper reaches of the Oujiang River Basin are divided into three sub watersheds (Figure 1b).

2.2 Precipitation

The gridded precipitation data come from the hourly precipitation data set of the National Meteorological Information Center, which integrates China's automatic station data with the NOAA CDR Climate Prediction Center morphing technique

(CMORPH) product with a resolution of 0.1°. The overall error is within 10%, and the accuracy in areas with heavy rainfall and sparse sites is greater than in similar international products (Shen et al., 2014). The data can effectively reproduce the spatiotemporal pattern of rainfall and are suitable for simulating flood inundation.

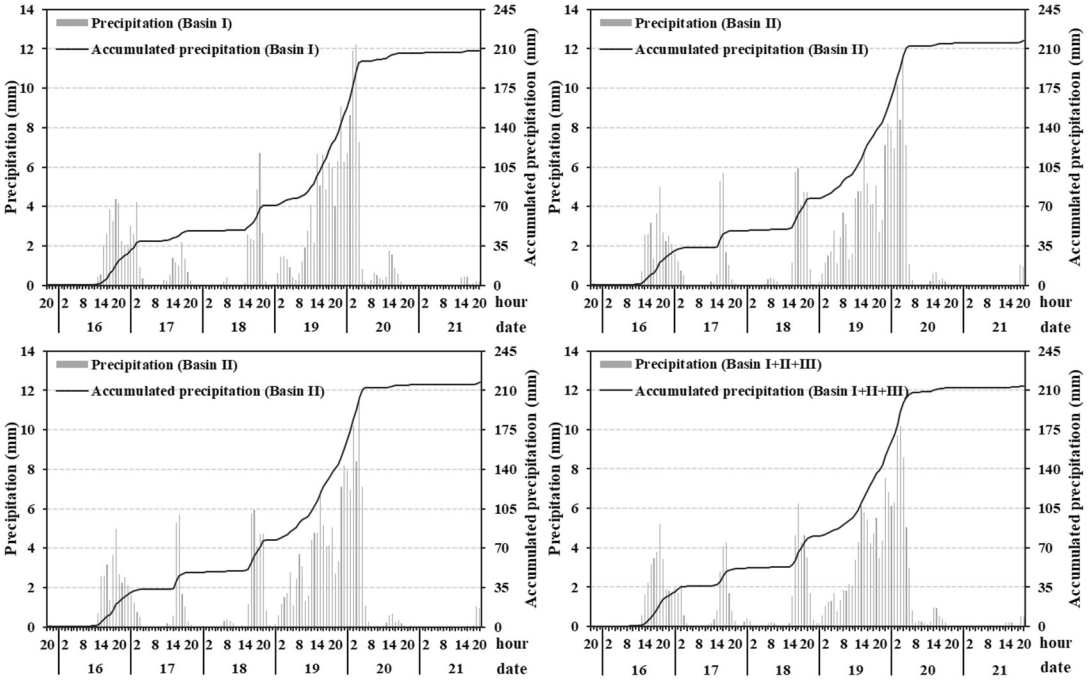

Figure 2. Distribution of hourly and accumulated precipitation in the upper reached of the Oujiang River Basin (Basin I + II + III)~~entire basin~~ and each sub_basin. (The grey column is hourly precipitation, and the black curve is ~~cumulative~~ accumulated precipitation. The precipitation time is from 20:00 on August 15th to 20:00 on August 21st, 2014.)

Based on the hourly precipitation levels, the mean accumulated precipitation of the ~~middle and~~ upper reaches of the Oujiang River Basin and the 3 sub watersheds were calculated (Figure 2). The precipitation change trend of each sub watershed ~~is~~was generally the same, with the accumulated precipitation exceeding 210 mm. The precipitation increased rapidly after 5:00 on August 18th, and the entire precipitation process basically ended at 10:00 on August 20th.

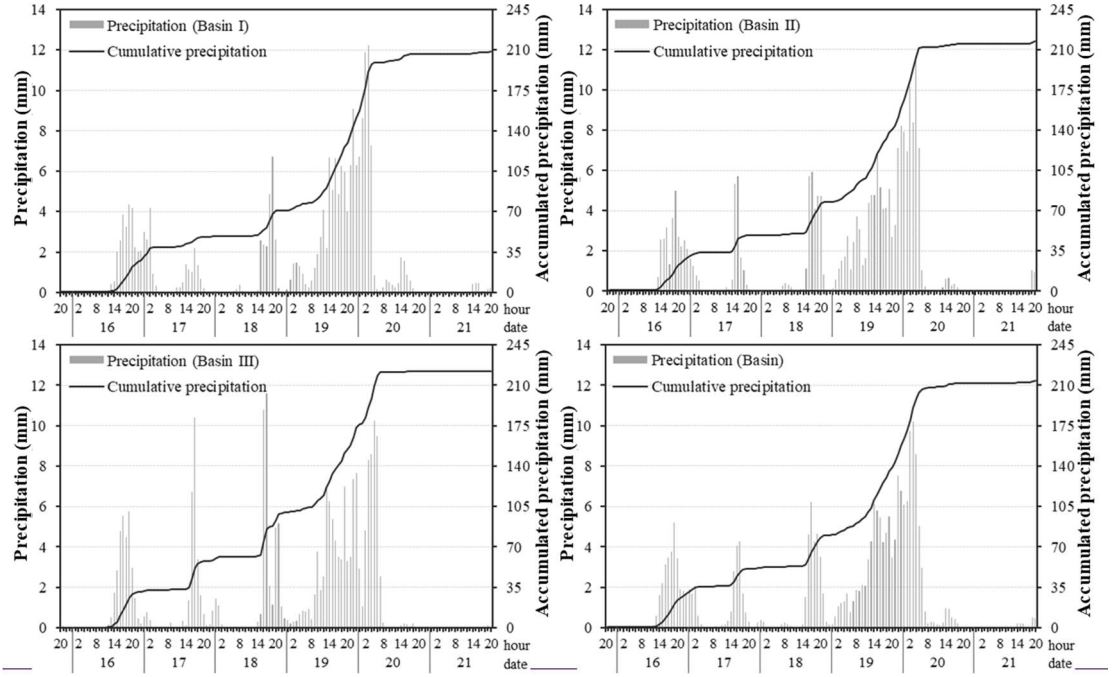

~~Figure 2. Distribution of hourly and accumulated precipitation in the entire basin and each subbasin. (The grey column is hourly precipitation, and the black curve is cumulative precipitation. The precipitation time is from 20:00 on August 15th to 20:00 on August 21st, 2014.)~~

2.3 Water level and flood inundation

The water level data come from the hourly observations of hydrological stations of the Zhejiang Water Resources Department, including the measured water level, warning water level, and guaranteed water level. Xiaobaiyan and Lishui are river stations, and the Jinshuitan Reservoir and the Kaitan Reservoir are reservoir stations (Figure 1). Based on the hourly measured water level, beginning at 12:00 on August 19th, the water levels of the Jinshuitan Reservoir, Xiaobaiyan, and Lishui increased significantly, while the water level of the Kaitan Reservoir first dropped slightly and then increased significantly, and the water levels at these stations reached a peak at approximately 12:00 on August 20th. The water levels at Xiaobaiyan, Lishui, and the Kaitan Reservoir returned to normal at 00:00 on August 21st, while that at the Jinshuitan Reservoir dropped to a certain water level at 00:00 on August 22nd, and the subsequent downward trend was slow (Figure 3).

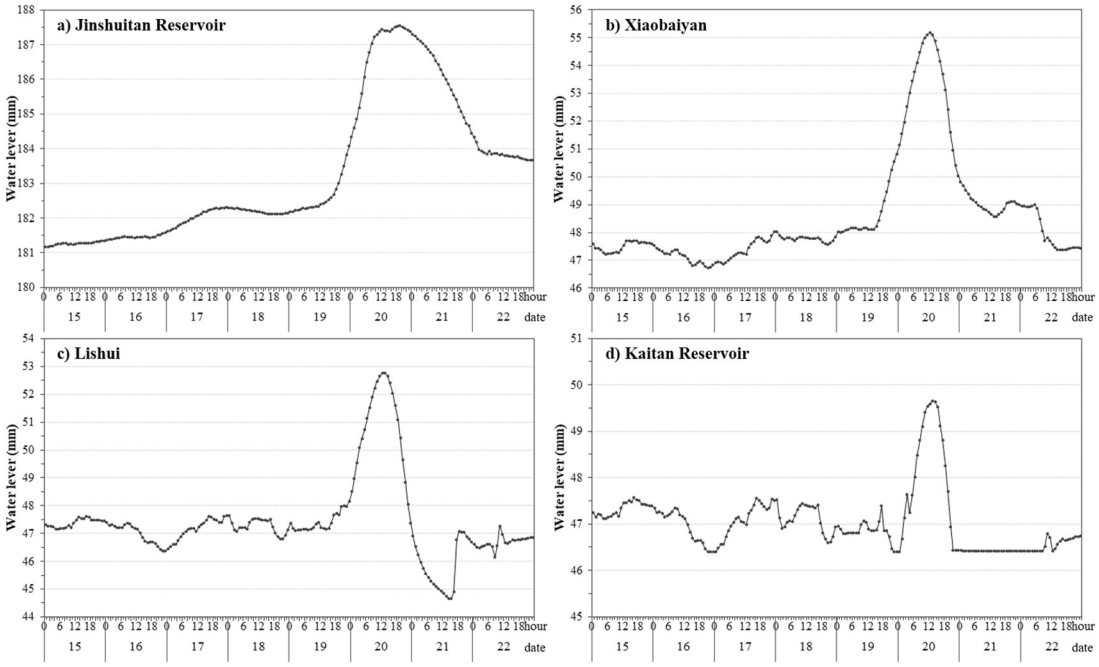

Figure 3. Distribution of hourly water levels at hydrological stations. (The time of water level data is from 00:00 on August 15th to 00:00 on August 23rd, 2014)

The flood inundation was calculated from the Yuxi to Kaitan Reservoir hydraulic model constructed by *Zhejiang Design Institute of Water Conservancy & Hydro-Electric Power*. ~~The~~In this study, the middle and upper reaches of the Oujiang River Basin were generalized into a mathematical model, the unsteady flow partial differential equations of the Saint-Venant open channel ~~are~~were used to ~~construct a one-dimensional hydrodynamic model. Then, based on the measured channel section, water level, reservoir discharge, and high-precision topography,~~ describe the flood evolution process, and the implicit difference method was used to transform it into a difference equation. Newton iteration and Gaussian principal component elimination method ~~are~~were used to solve the problem time by time, so as to obtain the water level and discharge of each section~~, and then the parameters are calibrated by the measured water level (Kang and Chen, 2007). After multiple verifications, the difference between the measured and calculated water levels was between 0 m and 0.09 m.~~(Kang and Chen, 2007). This model considered weirs, gates, water-blocking bridges, water exchange between intervals, and flood detention areas, etc., and can be applied to the quantitative analysis and calculation of the flood evolution of this section of the river.

In order to make the flood evolution calculation can better simulate the water depth of this basin, the measured river section and the flood in 2014 were selected for simulation calculation to verify the accuracy of the mathematical model of the flood evolution calculation, and determine the parameters of the model. The simulation result of the measured flood on August 20, 2014 was carried out. The upper boundary used the discharge process of each reservoir and the measured data from the hydrological station, and the lower boundary used the measured water level. Comparing the model result with the measured flood traces and the measured process at the hydrological station, the difference in water level between the two was 0 m - 0.09

m, which shows that the model parameters were reasonable. The flood volume was calculated based on the simulated water level and the elevation of the embankment (~~Table 1). When compared with the site survey and flood traces, the result is similar to the actual submerged depth.~~Table 1). Based on the overflow volume and topographic data, the submerged area and inundation depth were estimated by GIS tools. Through measured flood traces, field surveys and aerial photograph, it was found that the simulated submergence results can well reflect the actual flood.

~~Based on the simulated maximum submerged depth distribution (Figure 4a) and real-time aerial photographs (Figure 4b, Figure 4c), the flood inundation area is mainly concentrated in the river confluence and both sides of the river, the submerged depth decreases from the river bank to both sides, and the submerged depth of the central island is generally greater than 7 m.~~

Table 1. Overflow volume of Liandu ~~District~~district in 2014 based on the hydraulic model (10,000 m^3)

	Da River South	Da River East	Da River North (Da River Section)	Da River North (Hao River Section)
Overflow volume	230.63	264.81	60.17	277.51

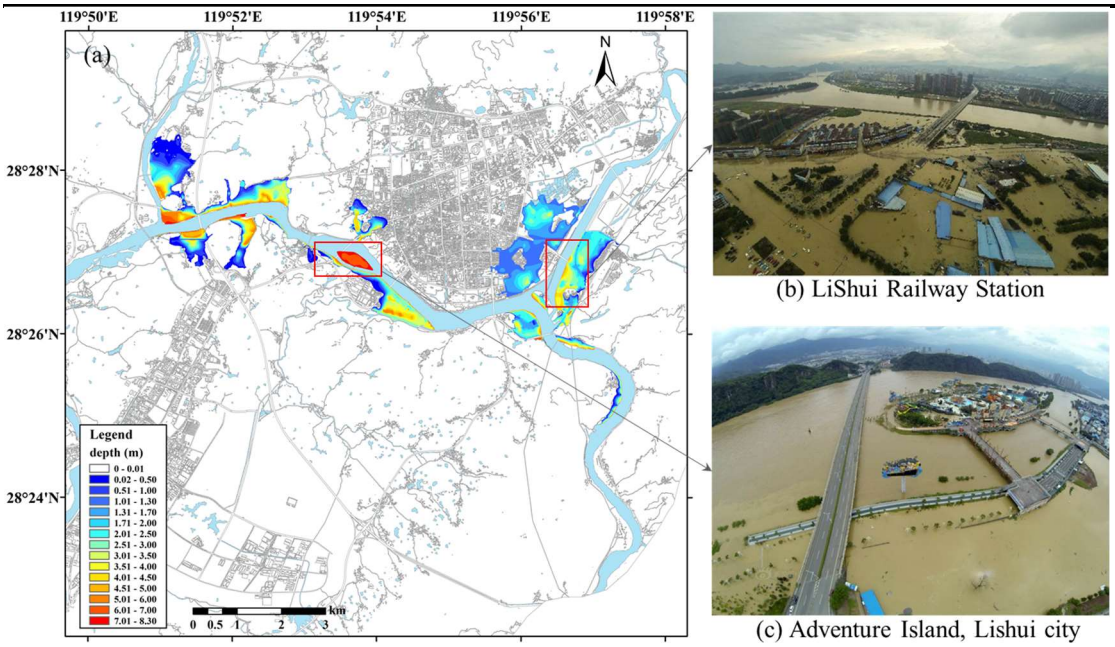

Figure 4. (a) ~~Maximum~~Distribution of maximum simulated submergence depth ~~distribution~~, (b, c) Aerial photographs of Liandu ~~District~~district in 2014.

Based on the simulated maximum inundation ~~submerged~~ depth distribution (Figure a) and real-time aerial photographs (Figure b, Figure c), the flood inundation area was ~~is~~ mainly concentrated in the river confluence and both sides of the river, the inundation ~~submerged~~ depth decreased ~~decreases~~ from the river bank to both sides, and the inundation ~~submerged~~ depth of the central island was ~~is~~ generally greater than 7 m.

2.4 Disaster loss reporting

The disaster loss report ~~is~~was obtained from the Lishui Civil Affairs Bureau ~~and is conveyed~~, which was reported by the local government. The report ~~records~~recorded 41 statistical indicators, including the affected population, affected area of crops, agricultural losses, infrastructure losses, public welfare facility losses, household property losses, and direct economic losses. According to these statistics, a total of 167,300 people ~~were~~was affected in Liandu, 17,330 people were relocated in emergencies, 247 rural houses collapsed, and the direct economic loss was approximately 377.15 million yuan.

The insurance claim ~~data come~~dataset came from the auto insurance list of the catastrophe "Zhejiang 0819 Rainstorm" of the Lishui branch of the People's Insurance Company of China (PICC), and the ~~data record~~dataset recorded 19 indicators, including the policy number, the information of the insured, the estimated compensation, and the compensation paid. As of August 24th, a total of 1,045 motor vehicle insurance reports were received, with a reported loss of 50.7969 million yuan and a decided compensation of 50.6893 million yuan. According to the analysis of the market share of various insurance types in Zhejiang Province in December 2014, PICC motor vehicle insurance accounted for approximately 48.357% of Lishui city.

3 Methods

In this study, an assessment model of the direct economic loss ratio and loss value of flood disasters was constructed by utilizing methods such as land use type fusion, land use value estimation, vulnerability curve fitting~~,~~ and optimization.

3.1 Data fusion of land use types

The distribution of land use types ~~is~~was obtained through the fusion of current land use data in Lishui city with ~~a high-precision~~high resolution land use classification results based on remote sensing ~~classification.~~data. The former data ~~come~~came from the urban and rural space development current status map of the Natural Resources and Planning Bureau in 2013, which ~~is divided into 47 categories according to the *Urban Land Classification and Planning and Construction Land Standards* (GB 50137-2011, 2011). The remote sensing classification is~~was divided into 47 categories (Table 2) according to the *Code for classification of urban land use and planning standards of development land* (MHURD, 2011). The land use classification results were derived from the Gaode map with a resolution of 2.3870768 m, including 5 categories: transportation, grassland, waters, agriculture and forest, and buildings. The fusion steps of vector data and raster ~~fusion~~data are as follows.

1) ~~The~~ First, we selected the unified geographic coordinate system ~~is adopted, the nearest neighbor method is~~ used in this study. In order to ~~resample~~ be consistent with the flood inundation results, we interpolated the land use classification results into raster data ~~onto~~with a ~~grid with a spatial~~ resolution of 2 m~~, and geometric correction and spatial registration are performed on~~ by the nearest neighbour interpolation method. Then the vectorized ~~land use data~~current land use data was spatial adjusted to make it overlap with the position of the land use classification results.

2) ~~The building pixels in the remote sensing classification are traversed, the~~Second, we extracted the land use type in the current land use data corresponding ~~current land type is queried by~~to the location of each building pixel in the land use classification result, and ~~the grid is reassigned using~~assigned the type~~.~~ to the corresponding building pixel. The building pixels

that have not been reassigned ~~are~~were assigned according to the adjacent building types. In addition, the road within 2 m of the residence ~~is~~was set as community parking, and the buildings far from urban areas ~~are~~were set as ~~rural residences~~the village construction land.

3) The water, agriculture and forest, and road in the ~~remote sensing~~land use classification ~~are~~results were assigned as water, agriculture and forest, and urban road, respectively. The agriculture and forest in areas with urban buildings and the agriculture and forest and grassland in park areas ~~are~~were assigned as park green land.

4) Whether there ~~are~~ were un-reassigned pixels in the ~~remote sensing~~land use classification ~~that have not been reassigned is checked.~~results. If so, these pixels were reclassified according to the corresponding current land type ~~is determined, and all pixels are classified~~.

3.2 Estimation of land use values

The value of land use obtained from expert questionnaires is relatively reliable, and the steps are as follows.

1) Based on the *Lishui City Master Plan* (2013-2030), *Lishui City 13th Five-Year Plan*, and *Lishui City Statistical Yearbook in 2015*, we gave the reference information ~~such as~~of current area, planned area, planned investment, unit area budget, and description of land use types ~~are given~~.

2) ~~As~~Due to the different disaster characteristics of land use, the four major categories of residential, commercial, ~~industrial,~~ public management~~,~~ and public services ~~are used to estimate the~~, and industrial were estimated the exposure value of the indoor properties, and the other categories were estimated the value or cost per unit area ~~is estimated for others.~~, as shown in Table 2.

3) ~~Questionnaires are~~We issued questionnaires to 7 experts in fields such as municipal engineering design, construction industry, water design, ecological city planning, and natural disasters, and invited experts ~~are invited~~ to estimate the land use value based on their professional background knowledge and the actual situation of the study area.

4) The value of each land use ~~is~~was determined by collating the questionnaires and calculating the average values.

3.3 Calibration of vulnerability curves

Although the vulnerability curves of different regions are different, there are similarities in the trend of the loss ratio with the ~~water depth, which we can learn from. Therefore, based on the existing vulnerability curves in many countries and regions (Coto, 2002; Dutta et al., 2003; FEMA, 2017; Mo and Fang, 2016; NRC, 2017; Reese and Ramsay, 2010; Shi, 2010; Wehner et al., 2017), the steps of vulnerability curve fitting~~inundation depth, and we can learn from them. Therefore, based on the existing vulnerability curves in many countries and regions (Coto, 2002; FEMA, 2013; Mo and Fang, 2016; Shi, 2010), the fitting and optimization steps of vulnerability function are as follows.

1) ~~The~~ According to the existing depth-damage database, the relationship between ~~the flooding~~inundation depth and loss ratio ~~is formulated~~ of each land use in Liandu ~~based on existing databases.~~ district was constructed. Since the HAZUS-~~Flood has~~FLOOD had a ~~relatively~~ complete ~~classification, so a mapping~~building occupancy class, this study mainly referred to it. First, we constructed the comparison table between the ~~database~~building occupancy class in HAZUS-FLOOD and the land

use type ~~of Liandu is established. The~~in Liandu district. Second, based on the inundation depth in Liandu district and the water depth in HAZUS-FLOOD, the range of inundation depth in the depth-damage function was set and the unit of water depth was converted to meters. Finally, the HAZUS-FLOOD was summarized according to the building occupation class, and the average loss ratio of ~~the corresponding type of HAZUS functions as a~~ all samples for each building occupancy class under each inundation depth was calculated, which was used as the reference ~~for~~of the loss ratio of ~~Liandu.~~corresponding land use types under the same inundation depth in Liandu district. If there ~~is~~was no similar building occupancy type in HAZUS-FLOOD, other databases ~~are~~were referenced~~.~~ (Figure 6).

~~2) The vulnerability curve can be fitted by a polynomial, a power function (Büchele et al., 2006), or logistic regression (Cao et al., 2016), and it can also be smoothed by nonparametric forms such as the kernel density (Merz et al., 2004). The lognormal cumulative distribution function (Limpert et al., 2001) with a high fitting degree is selected to fit the vulnerability curve, and the formula is as follows:~~

2) The appropriate function was selected to fit the curve of inundation depth and loss ratio for each land use type constructed in step 1. In the previous study, the vulnerability curve can be fitted by a polynomial, a power function (Büchele et al., 2006), or logistic regression (Cao et al., 2016), and it can also be smoothed by nonparametric forms such as the kernel density (Merz et al., 2004). In this paper, the lognormal cumulative distribution function (Limpert et al., 2001) was selected to fit the vulnerability curve. The formula is as follows:

$$y = F(x, scale, shape) = F(x|\mu,\sigma) = \frac{1}{\sigma\sqrt{2\pi}}\int_0^x \frac{1}{t} e^{\frac{-(\log t-\mu)^2}{2\sigma^2}} dt, \quad x > 0 \tag{1}$$

where ~~F~~y is the ~~direct economic~~ loss ratio, x is the ~~submerged~~inundation depth, ~~and~~ σ and μ are the standard deviation and mean of the ~~logarithm of~~ ~~x~~$logx$, respectively. For lognormal cumulative distribution function F, the shape parameter $shape = \sigma$, which affects the shape of the distribution, and scale parameter $scale = e^{\mu}$, which affects the stretching and shrinking of the distribution.

3) Based on the ~~fitted~~ vulnerability ~~curve of land use~~function fitted in step 2, the loss ratio ~~is calculated by~~and loss value of land use in Liandu district were estimated. First, the two ~~attributes of the submerged depth and~~raster layers of land use type~~.~~ and inundation depth were overlaid. Then, the loss ~~value is~~ratio of each grid was calculated based on the ~~loss ratio and land use value, and the formula is as follows:~~vulnerability function. If the inundation depth of the grid was 0 m, the loss ratio was also 0. Otherwise, the corresponding vulnerability function was searched according to the land use type of the grid, and its loss ratio was calculated based on the inundation depth of the grid. Finally, the loss value of each grid was calculated by Eq. 2.

$$L = DR * V \tag{2}$$

where L is the loss value of the land use, DR is the loss ratio of the land use, and V is the value of the land use.

4) ~~Based on the~~ The vulnerability function was optimized by disaster loss reporting data. First, the mapping ~~relationships~~table between the ~~disaster~~ statistical indicators of disaster loss reporting and land use types in Liandu district was constructed (Table 2). Second, the simulated ~~direct economic losses are summarized, and~~ total loss of land use in Liandu district corresponding to the ~~nonlinear~~loss reporting data of indicator k was calculated by Eq. 3. Then, the non-linear equation

~~is~~was established with the minimum error ~~of~~between the disaster ~~statistical~~reporting loss and the simulated total loss as the objective function~~. The~~, and the scaling factor a_k was solved by the least square method ~~is~~.

$$TL_k = \sum_{i=1}^{n_k} \sum_{j=1}^{m_{ik}} L_{ij} = \sum_{i=1}^{n_k} \sum_{j=1}^{m_{ik}} F\left(x_{ij}, shape_i, a_k * scale_i\right) * value_i \quad (k = 1,2, \dots ,5) \quad (3)$$

where TL_k is the simulated total loss, n_k is the number of land use types corresponding to the disaster loss reporting indicator k, m_{ik} is the number of grids of the land use type i corresponding to the indicator k, L_{ij} and $F\left(x_{ij}, shape_i, a_k * scale_i\right)$ are the loss value and loss ratio of the grid j of the land use type i, respectively. $value_i$ is the asset value or cost per unit area of land use type i, x_{ij} is the inundation depth of the grid j of the land use type i, $shape_i$ and $scale_i$ are the parameter of the vulnerability function of the land use type i, a_k is the scaling factor of the indicator k, and the initial value is 1.

5) Based on the optimized vulnerability function, we used ~~to solve the nonlinear equation to optimize the scale parameters, and then the optimized vulnerability curve is used~~the method in step 3 to re-estimate the ~~disaster loss~~loss ratio and loss value of land use in Liandu district.

4 Results and Analysis

4.1 Distribution of land use types

The distribution of high-resolution land use types in Liandu ~~is~~was obtained by ~~implementing~~using the data fusion method (Figure 5a), and the names and codes of land use types ~~are~~were shown in Table 2. The fused land use type data effectively integrate the ~~corresponding~~respective advantages of the current urban land use and land use classification results based on remote sensing ~~classification~~images. The data not only have high-resolution spatial location information but also reflect the detailed types of land use.

Agricultural and forestry land in Liandu ~~District~~district is the most widely distributed type. Woodlands are mainly distributed in the hilly areas of the north, east, south, and northeast. The built-up area of Liandu ~~District~~district is distributed along the river in a block shape, among which residential land is mainly distributed in communities near the river. Industrial land is mainly distributed in ~~northeastern~~north-eastern Wanxiang Street and the Economic and Technological Development Zone, which is currently in the development stage, and many industrial plants have been built.

To strengthen intraregional connections, the roads and traffic facilities are relatively complete, with an urban road area of 4.33 km^2. Commercial, warehouse, public management, and public service facilities are relatively small and scattered. They are mainly concentrated near residential and industrial land, providing various services. Park green space is distributed along the river or close to residential and commercial land, while square green space, protective green space, and public facilities are small and scattered.

4.2 Distribution of land use values

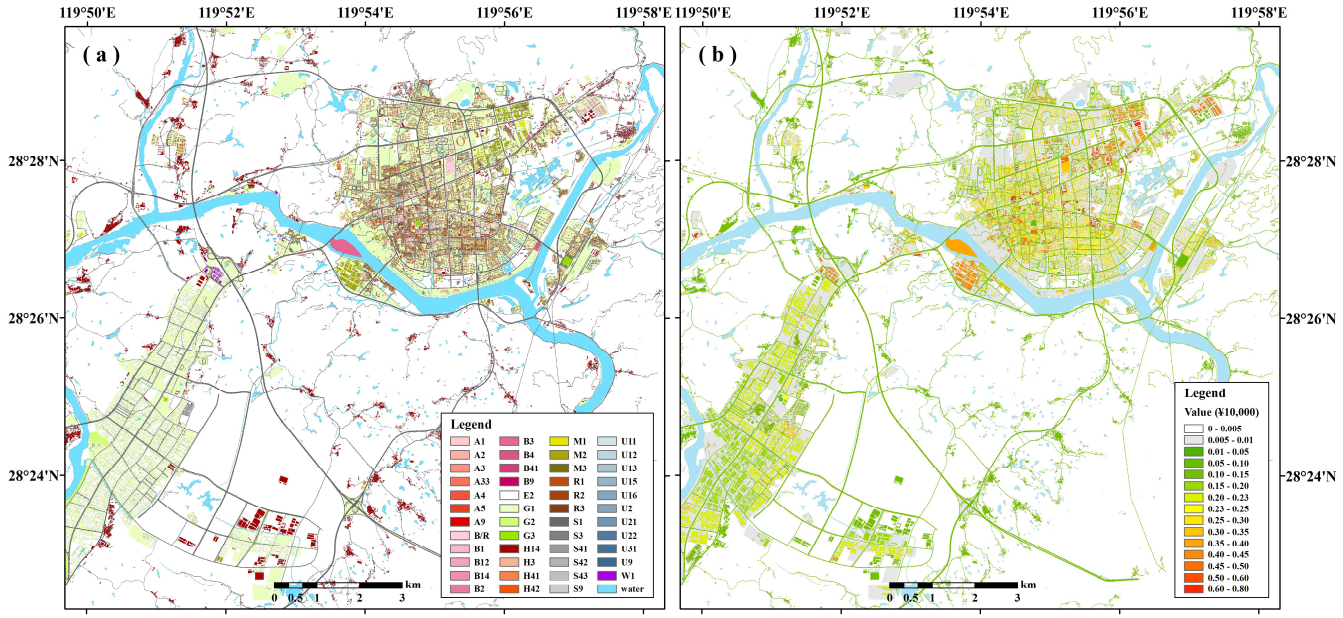

~~**Figure 5. Distribution of land use types (a) and land use values (b) in the central urban area of Liandu District in 2013.**~~

The asset value or cost per unit area of land use types ~~is~~was estimated based on expert questionnaires (Table 2). Commercial and industrial land has many internal equipment and items with the highest asset unit price. Public management and public service facilities and residential land have a higher indoor property value. The value of agricultural and forestry land is the lowest.

The spatial distribution of land use value in Liandu in 2013 ~~is~~was calculated through grid assignment (Figure 5b). The value of assets per unit area in the northern city and Wanxiang Street is generally high due to the concentration of commercial, industrial, residential, public management, and public service facilities in the area. There is a water amusement project on the central island, which has a higher value per unit area. Many industrial plants are distributed in the Economic and Technological Development Zone, but due to the development stage and incomplete internal facilities, the unit price of the industrial land in this zone is calculated at half of the estimated value. Agricultural and forestry land is widely distributed and low in value, so most areas of Liandu have low values.

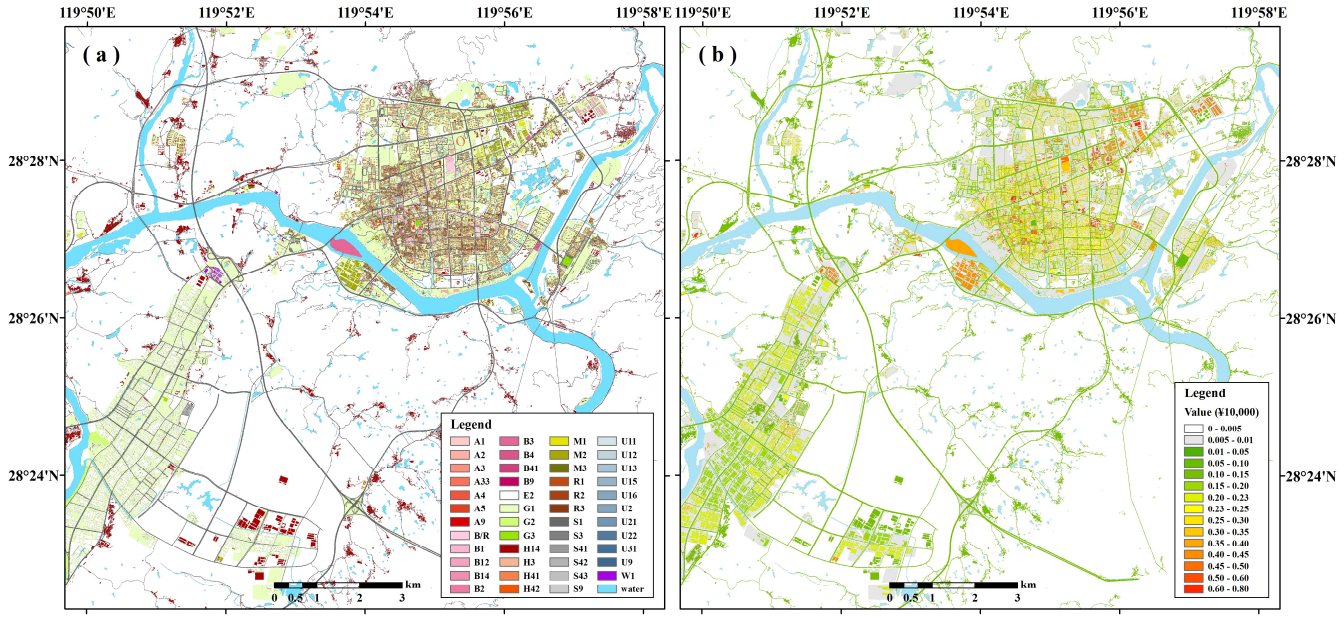

Figure 5. Distribution of land use types (a) and land use values (b) in the central urban area of Liandu district in 2013.

4.3 Fitted vulnerability curves

The vulnerability curves of all land use types ~~are~~were fitted by a lognormal cumulative distribution function based on the matrix of the ~~submerged~~inundation depth and loss ratio. ~~By comparing~~Based on the comparison of simulated losses and disaster loss ~~reporting~~report data (Table 2), we optimized the scale ~~parameter~~parameters of the vulnerability ~~curve is optimized~~ function (Figure 6) through the ~~least square~~vulnerability curve calibration method ~~(Figure 6).~~(Section 3.3).

~~The loss ratios of residential, industrial, commercial, warehousing, public management, and public service land are very high, mainly due to indoor properties being soaked or washed away by floods. As the submerged depth increases, the loss ratio increases rapidly. When the depth is higher than 3 m, the loss ratio increases, and the rate of increase is unclear.~~

Table 2 The Classification, value, inundated area of land use types, and the comparison of simulated loss before optimization, simulated loss after optimization and statistics loss of each land use type in Liandu ~~District~~district.

Code	Classification	Value (¥10,000/4 m^2)	Total value (¥10,000)	Inundated area (m^2)	Mean loss ratio of inundated area	Simulation loss before optimization (¥10,000)	Simulation loss after optimization (¥10,000)
A1*	administrative office	0.40	~~13891.60~~13,892	~~20202~~,020	0.79	160.~~41~~	~~130.81~~131
A2*	cultural facilities	0.35	~~3309.60~~3,310	24	0.81	1.~~71~~7	1.~~31~~1
A3*	educational and scientific research	0.25	~~13914.00~~13,914	~~15980~~15,980	0.64	639.~~38~~	~~499.98~~500
A33*	primary and secondary schools	0.20	~~5946.60~~5,947	~~72967~~,296	0.31	~~111.98~~112	77.~~36~~
A4*	sports land	0.30	~~1311.45~~1,311	0	0.00	0.~~00~~	0.~~00~~

A5*	medical and health land	0.35	4601.274,601	568	0.80	39.8240	31.7232
A9*	religious land	0.10	288.70289	0	0.00	0.00	0.00
B/R*	commercial and residential land	0.35	8415.998,416	144	0.45	5.667	1.879
B1*	commercial facilities	0.46	9944.749,945	59085,908	0.89	602.53603	473.27
B12*	wholesale market land	0.50	15358.2515,358	1625216,252	0.48	981.98982	457.98458
B14*	hotel land	0.30	3247.503,248	25202,520	0.29	54.5155	19.38
B2*	business facilities	0.60	11071.8011,072	11001,100	0.10	16.17	2.00
B4*	business outlets of public facilities	0.35	18.519	148	0.47	6.15	3.20
B41*	gas station	0.44	249.70250	0	0.00	0.00	0.00
B9*	other service facilities	0.23	350.06	23082,308	0.64	84.37	48.19
M1*	class I industrial	0.60	20913.6020,914	336	0.81	40.9241	30.04
M2*	class II industrial	0.40	146229.20146,229	3259232,592	0.52	1692.031,692	1059.571,059
M3*	class III industrial	0.30	39283.5039,284	1013210,132	0.55	418.00	237.72238
W1*	Warehouse	0.50	7500.007,500	79047,904	0.85	836.18	606.79607
E2**	agriculture and forest	0.004	1398391.701,398,392	39432243,943,224	0.65	637.25	637.25
R1*	class I residential	0.35	3312.053,312	0	0.00	0.00	0.00
R2*	class II residential	0.25	104612.25104,612	232924232,924	0.53	7666.897,667	9435.069,435
R3*	class III residential	0.20	35893.5035,894	7867278,672	0.70	2756.772,757	3189.113,189
H14*	village construction	0.13	425820.70425,821	176868176,868	0.78	4507.904,508	5189.185,189
S43*	community parking	0.50	63235.5063,236	6646866,468	0.75	6191.586,192	7266.657,267
H3**	regional public facilities	0.15	349.80350	0	0.00	0.00	0.00
H41**	military sites	0.30	629.70630	0	0.00	0.00	0.00
H42**	security	0.08	467.60468	0	0.00	0.00	0.00
S1**	urban road	0.12	1055377.421,055,377	931240931,240	0.07	2047.783,048	2141.033,141
S3**	transportation hub	0.28	5559.965,560	45924,592	0.08	25.16	26.12
S41**	public transport station	0.40	0.808	0	0.00	0.00	0.00
S42**	social parking	0.60	2106.602,107	0	0.00	0.00	0.00
S9**	other transportation facilities	0.15	284.70285	4	0.44	0.07	0.07
U11**	water supply	0.27	857.25	0	0.00	0.00	0.00
U12**	power supply	0.30	930.90931	8	0.06	0.04	0.04
U13**	gas supply	0.40	108.40	0	0.00	0.00	0.00
U15**	communication facilities	0.80	3294.403,294	0	0.00	0.00	0.00
U16**	radio and television facilities	0.80	808.80809	0	0.00	0.00	0.00
U2**	environmental facilities	0.50	140.50141	0	0.00	0.00	0.00
U21**	drainage facilities	0.45	757.35	33523,352	0.25	94.22	96.50
U22**	sanitation facilities	0.15	197.40	544	0.17	3.444	3.535
U31**	fire control facilities	0.30	727.20	0	0.00	0.00	0.00

U9**	other public facilities	0.15	21.00	0	0.00	0.00	0.00
G2**	protection greenbelt	0.01	713.15	0	0.00	0.00	0.00
G3**	square land	0.08	1178.961179	2819228,192	0.41	230.11	233.69234
G1**	park green space	0.01	48264.8948,265	16080961,608,096	0.55	2211.922,212	2211.922,212
B3*	recreational and sports facilities	0.38	18234.6818,235	161216161,216	0.88	13540.9513,541	13540.9513,541

* The estimated exposure value is the indoor property value; ** the estimated value is the value or cost per unit area.

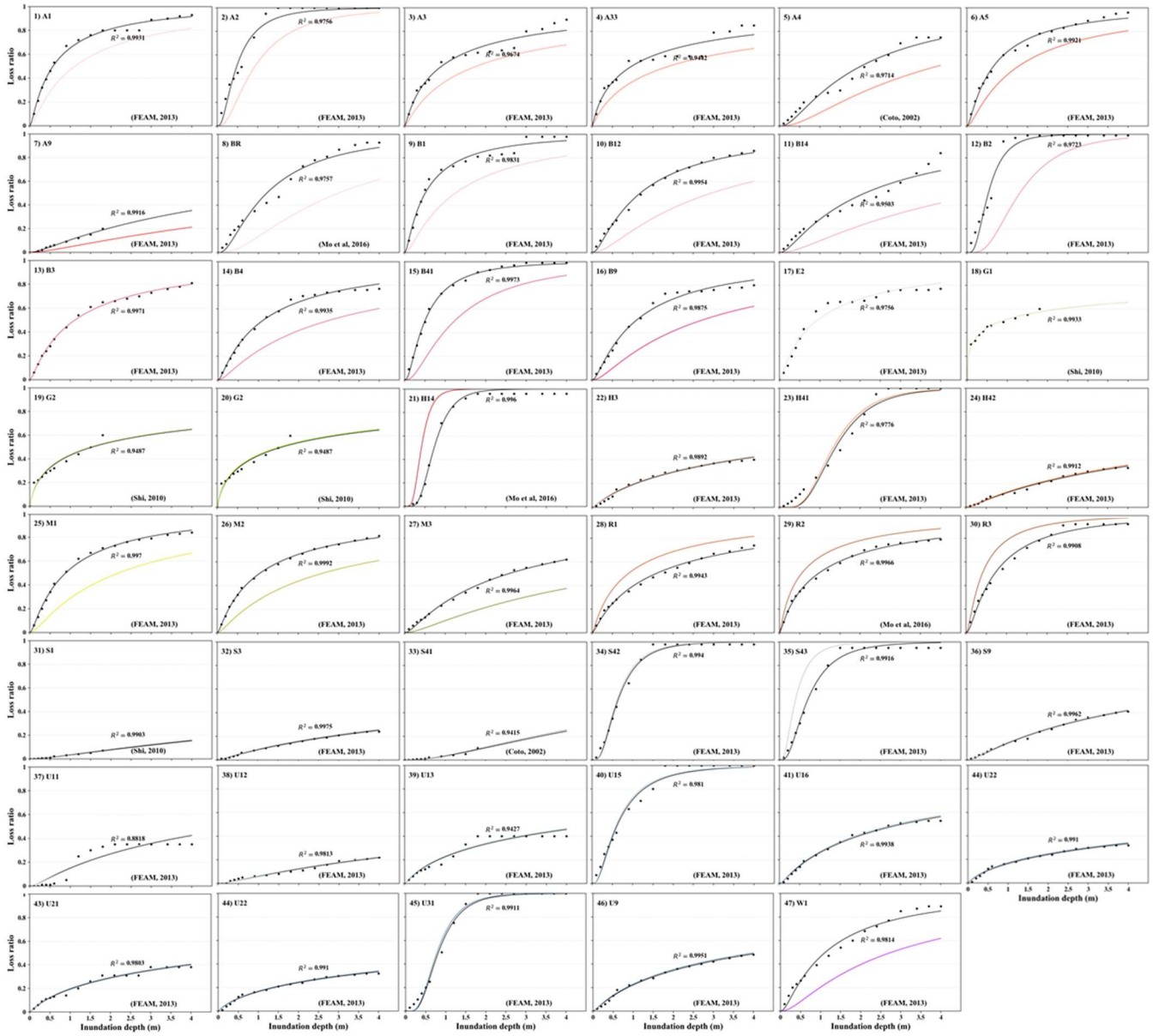

Figure 6. Fitting and optimization of vulnerability curves of land use in Liandu ~~District~~ district (The black dots refer to the inundation depth and loss ratio based on the reference, the ~~The~~ black curve is the fitting result of the black dots by the lognormal CDF, and the color curve is the optimized result based on the disaster loss reporting).

The loss ratios of residential, industrial, commercial, warehousing, public management, and public service land are very high, mainly due to indoor properties being soaked or washed away by floods. As the inundation depth increases, the loss ratio increases rapidly. When the depth is higher than 3 m, the increase of loss ratio is not obvious.

The direct impact of floods on public facilities and roads is relatively small, and the loss ratio is generally low. However, the indirect loss caused by the suspension of roads, communications, and electricity is relatively large but is not calculated in this study. Green space and square land are less affected by floods, and the loss ratio is relatively low.

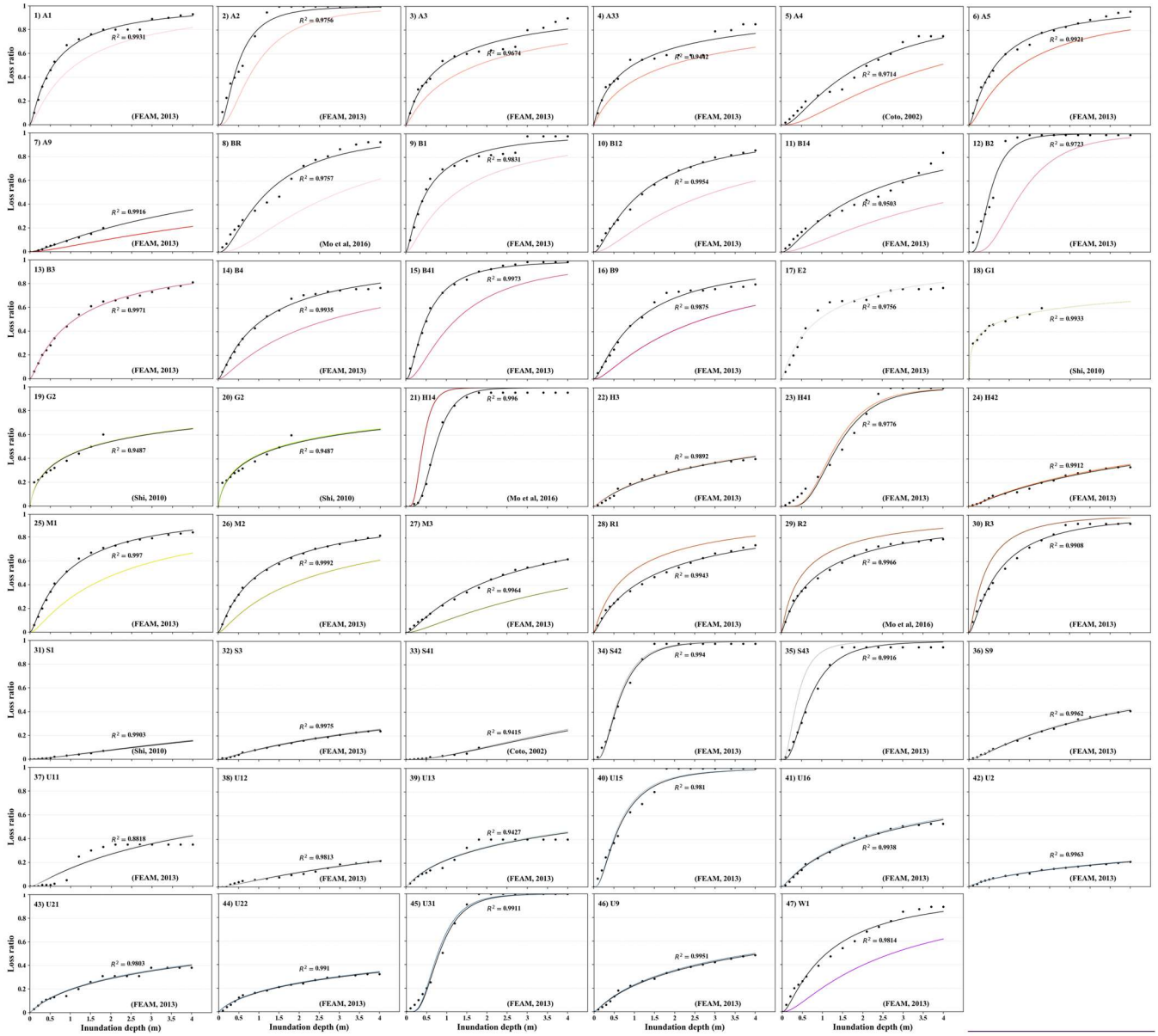

~~Figure 6. Fitting and optimization of~~ The scale parameters of the vulnerability ~~curves~~curve of the land use type corresponding to each statistical indicator in ~~**Liandu District (The black curve is the fitting result, and the color curve is**~~ disaster report selected the ~~**optimized result).**~~

~~The~~ same optimization ~~coefficients are selected for~~ coefficient, and the ~~scale parameters of the same type of land use vulnerability curve and are~~coefficient was obtained by solving the nonlinear ~~equations~~equation. The vulnerability curve of family property is stretched, that of infrastructure is stretched slightly, and those of public welfare facilities, industry, and commerce shrink. This comparison shows that the simulated loss after optimization is consistent with the disaster loss reporting, and the optimization effect is good (Table 2).

4.4 Distributions of the loss ratio and loss value

~~The loss ratio (Figure 7a) and loss value (Figure 7b) distributions of the flood disaster in Liandu District are obtained based on a spatial analyst algorithm.~~

Based on the land use type and value data, the inundation depth distribution, and the optimized vulnerability functions of the land use, the distribution of loss ratio (Figure 7a) and loss value (Figure 7b) of Liandu district were estimated by the method in step 3 of Section 3.3.

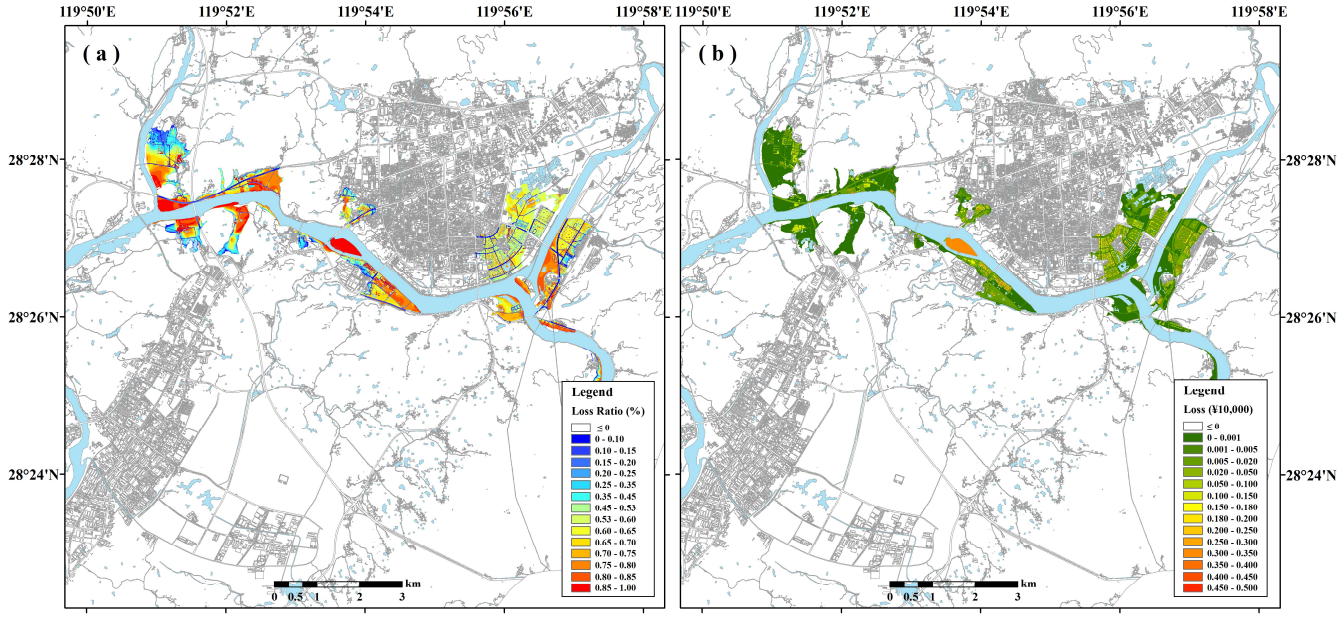

Figure 7. Spatial distribution of the flood loss ratio (a) and loss values (b) in the central urban area of Liandu ~~District~~district in 2014.

Due to the high inundation depth at the river confluence and both sides of the river as well as the wide distribution of agricultural land in the area, the mean loss ratio of these areas is approximately 0.63. The ~~submerged~~inundation depth of the island is more than 7 m, and there are entertainment facilities on it, so the loss ratio is more than 0.6. In addition, the ~~submerged~~inundation depth on both sides of the Hao River is more than 1 m. The west side of the river is mainly residential land, and the east side is the Lishui railway station, so the indoor property loss ratio is high. However, traffic land is less directly affected by floods, so the loss ratio is less than 0.2 (Figure 7a).

The loss value of a flood disaster is affected by the unit value and loss ratio of the land use. Therefore, the distribution characteristics of the loss ~~rate~~ratio and loss value are different. The loss ratio of this flood is relatively high, but due to the wide distribution of agricultural land in the submerged area, the loss value per unit area is low. The loss ratio and unit area value of recreational and sports facilities, residential, industrial, commercial, public management, and public service facilities are high, so the loss values are also high. The loss ratio of traffic facilities is very low, yet the loss value is relatively high due to the high construction cost (Figure 7b).

Liandu ~~District~~district is surrounded by high mountains, and the overland flow, affected by the topography, was formed by rainfall flowing into the Da River through the rivers in the north. The occurrences of heavy rainfall in the middle and upper reaches of the Oujiang River are similar, causing the whole basin to experience the flood peak period at the same time, which is not conducive to flood diversion efforts. To relieve the flood pressure on the basin, the Jinshuitan Reservoir was opened twice. At the same time, rapid urbanization has brought about great changes in the morphology of river channels and waters. These factors caused the river's water level to rise rapidly, overtopping the flood dyke and submerging low-lying areas along the riverbed. In addition, due to the high population density and highly concentrated economy in the northern area of Liandu ~~District~~district, serious economic losses will inevitably occur when floods exceed the fortification standard of dyke.

5 Conclusion and discussion

The research and verification of the refined assessment of single-flood disaster loss was carried out by utilizing the refined types and values of land use and quantitative vulnerability curves, and the main conclusions are as follows.

The 47 types of land use ~~type~~ data obtained by the fusion of vector and raster data overcome the limitations of the original data. This procedure not only refines the data into detailed urban land use types but also has a high spatial resolution. In addition, in the absence of a comprehensive and detailed survey of exposure data, the unit area costs or asset values obtained through the collection of written ~~sources and a survey of experts via~~materials and expert questionnaires can reflect the overall distribution of the value of the exposure data to a ~~questionnaire are more reasonable.~~certain extent. The ~~land use~~ types and values of land use constructed by the above methods provide ~~fine~~precise and reasonable ~~disaster-bearing body~~exposure data for ~~a~~the refined assessment of disaster losses~~, thus laying a data foundation~~.

Based on lognormal cumulative distribution function fitting and scale parameter optimization, the vulnerability curves of 47 land use types ~~of disaster-bearing bodies~~ accurately reflect the characteristics of ~~the~~land use loss ratio ~~of the disaster-bearing bodies~~ varying with the ~~submerged~~inundation depth in Liandu ~~District~~district and provide a reliable ~~stage~~depth damage function curve for refined loss assessment. Among these ~~disaster-bearing bodies~~land use types, residential, industrial, commercial, public management, and storage land are seriously affected by flooding. Other land uses are relatively less affected, and the loss ratio increases slowly. In the absence of a large amount of post-disaster field survey data, the method proposed in this study can be used to construct vulnerability curves in accordance with the regional situation.

A refined assessment model of the direct economic loss of a single flood disaster is constructed in accordance with the regional characteristics based on the refined research and verification of each link in the disaster loss assessment. The estimated spatial distributions of the loss ratio and loss value of the flood disaster accurately reflect the intensity and spatial pattern of disaster loss ~~and provide scientific guidance for disaster prevention, mitigation,~~, which is conducive to the government's rational deployment of rescue forces and effective emergency ~~rescue. In addition to~~assistance, especially in areas with severe disasters to increase rescue forces and evacuate the people in time to reduce losses to a certain extent. Expect for park green space, recreational and sports facilities, and agricultural and forestry land, the ~~losses~~total loss of other land use types after

optimization ~~are consistent with the loss reporting~~is 322.6 million yuan, which is 510,000 yuan higher than the loss report data. The error between the two is relatively small, indicating that the loss assessment model of this study can be effectively applied to this area.

The loss assessment model constructed in this study can be used to estimate flood disaster losses under ~~different~~various climate change and socio-economic ~~development~~ scenarios, providing a basis for flood risk assessment and management in small- and medium-sized cities. This, in turn, will help the government formulate reasonable climate adaptation policies and sponge city planning~~.~~ (MHURD, 2014).

In this study, only the inundation and disaster loss reporting of one precipitation event are collected, thereby affecting, to a certain extent, the optimization results of the vulnerability curves. In the future, the data of several precipitation events will be collected to better calibrate the vulnerability curves and render the final optimized vulnerability curves more suitable for the region. Furthermore, the flood disaster caused serious direct economic losses to Liandu ~~District~~district. The disaster also stimulated a large amount of disaster relief investment, even as it disrupted public services and traffic, caused production losses for companies outside the flooded area, reduced agricultural production, and affected related industries ~~(Jonkman et al., 2008)~~(Jonkman et al., 2008). Therefore, it is necessary to carry out further research regarding the refined assessment of the indirect economic losses of flood disasters.

Code and data availability. The data used in the study are available at https://github.com/Haixia-Zhang/Flood-loss-assessment.git

Author contributions. ~~ZHX~~FWH and ~~FWH~~ZHX conceived the research framework and developed the methodology. ZHX was responsible for the code compilation, data analysis, graphic visualization, and first draft writing. FWH managed the implementation of research activities and revised the manuscript. ZH ~~collected~~participated in the data ~~for~~collection of this study. All authors discussed the results and contributed to the final version of the paper.

Competing interests. The authors declare that they have no conflict of interest.

Special issue statement. This article is part of the special issue “Advances in flood forecasting and early warning”. It is not associated with a conference.

Acknowledgements. This work was mainly supported by the National Key Research and Development Program of China (grant nos. 2018YFC1508803 and 2017YFA0604903), and the Key Special Project for Introduced Talents Team of Southern Marine Science and Engineering Guangdong Laboratory (Guangzhou) (No. GML2019ZD0601). The authors would like to acknowledge Kang Ying and Lin Song of the *Zhejiang Design Institute of Water Conservancy & Hydro-Electric Power* for providing the ~~simulation~~flood inundation ~~of flooding model~~data in Liandu ~~District~~district.

Financial support. This research has been supported by the National Key Research and Development Program of China (grant nos. 2018YFC1508803 and 2017YFA0604903), and the Key Special Project for Introduced Talents Team of Southern Marine Science and Engineering Guangdong Laboratory (Guangzhou) (grant no. GML2019ZD0601).

References

Albano, R., Sole, A., Adamowski, J., Perrone, A. and Inam, A.: Using FloodRisk GIS freeware for uncertainty analysis of direct economic flood damages in Italy, Int. J. Appl. Earth Obs. Geoinf., 73(February), 220–229, doi:10.1016/j.jag.2018.06.019, 2018.

Alfieri, L., Feyen, L. and Di Baldassarre, G.: Increasing flood risk under climate change: a pan-European assessment of the benefits of four adaptation strategies, Clim. Change, 136(3–4), 507–521, doi:10.1007/s10584-016-1641-1, 2016.

Amadio, M., Mysiak, J., Carrera, L. and Koks, E.: Improving flood damage assessment models in Italy, Nat. Hazards, 82(3), 2075–2088, doi:10.1007/s11069-016-2286-0, 2016.

Büchele, B., Kreibich, H., Kron, A., Thieken, A., Ihringer, J., Oberle, P., Merz, B. and Nestmann, F.: Flood-risk mapping: contributions towards an enhanced assessment of extreme events and associated risks, Nat. Hazards Earth Syst. Sci., 6(4), 483–503, doi:10.5194/nhess-6-485-2006, 2006.

Cao, S., Fang, W. and Tan, J.: Vulnerability of building contents to coastal flooding based on questionnaire survey in Hainan after typhoon Rammasun and Kalmeagi, J. Catastrophology, 31(2), 188–195, doi:https://doi.org/10. 3969 /j. issn.1000-811X.2016.02.036, 2016.

Carisi, F., Schröter, K., Domeneghetti, A., Kreibich, H. and Castellarin, A.: Development and assessment of uni- and multivariable flood loss models for Emilia-Romagna (Italy), Nat. Hazards Earth Syst. Sci., 18(7), 2057–2079, doi:10.5194/nhess-18-2057-2018, 2018.

Coto, E. B.: Flood hazard, vulnerability and risk assessment in the city of Turrialba, Costa Rica, International Institute for Geo-information Science and Earth Observation(ITC), Enschede, The Netherlands. [online] Available from: http://www.itc.nl/library/Papers/msc_2002/ereg/badilla_coto.pdf, 2002.

Custer, R. and Nishijima, K.: Flood vulnerability assessment of residential buildings by explicit damage process modelling, Springer Netherlands., 2015.

Dutta, D., Herath, S. and Musiake, K.: A mathematical model for flood loss estimation, J. Hydrol., 277~~(1–2),~~ 24–49, doi:10.1016/S0022-1694(03)00084-2, 2003.

Elkhrachy, I.: Flash Flood Hazard Mapping Using Satellite Images and GIS Tools: A case study of Najran City, Kingdom of Saudi Arabia (KSA), Egypt. J. Remote Sens. Sp. Sci., 18(2), 261–278, doi:10.1016/j.ejrs.2015.06.007, 2015.

EMA: Disaster loss assessment guidelines, Part III, Emergency management practice, Volume 3, guidelines, Canberra, Emergency Management Australia (EMA)., 2002.

Falter, D., Schröter, K., Dung, N. V., Vorogushyn, S., Kreibich, H., Hundecha, Y., Apel, H. and Merz, B.: Spatially coherent flood risk assessment based on long-term continuous simulation with a coupled model chain, J. Hydrol., 524, 182–193, doi:10.1016/j.jhydrol.2015.02.021, 2015.

FEMA~~:~~ (Federal Emergency Management Agency): Multi-hazard ~~Loss~~loss estimation methodology. ~~Flood Model,~~ HAZUS-MH flood model technical manual., ~~2017~~2013.

Gerl, T., Kreibich, H., Franco, G., Marechal, D. and Schröter, K.: A review of flood loss models as basis for harmonization and benchmarking, PLoS One, 11(7), doi:10.1371/journal.pone.0159791, 2016.

Hasanzadeh Nafari, R., Ngo, T. and Lehman, W.: Calibration and validation of FLFArs-A new flood loss function for Australian residential structures, Nat. Hazards Earth Syst. Sci., 16(1), 15–27, doi:10.5194/nhess-16-15-2016, 2016a.

Hasanzadeh Nafari, R., Ngo, T. and Lehman, W.: Development and evaluation of FLFAcs - A new Flood Loss Function for Australian commercial structures, Int. J. Disaster Risk Reduct., 17, 13–23, doi:10.1016/j.ijdrr.2016.03.007, 2016b.

Hsu, W.-K., Huang, P.-C., Chang, C.-C., Chen, C.-W., Hung, D.-M. and Chiang, W.-L.: An integrated flood risk assessment model for property insurance industry in Taiwan, Nat. Hazards, 58(3), 1295–1309, doi:10.1007/s11069-011-9732-9, 2011.

Jonkman, S. N., Bočkarjova, M., Kok, M. and Bernardini, P.: Integrated hydrodynamic and economic modelling of flood damage in the Netherlands, Ecol. Econ., 66(1), 77–90, doi:10.1016/j.ecolecon.2007.12.022, 2008.

Kang, Y. and Chen, Z.: Simulation model of water resources allocation in plain river network area, Water Resour. Prot., 23(5), 31-34+37, doi:https://doi.org/10.3969/j.issn.1004-6933.2007.05.009, 2007.

Koks, E. E., Jongman, B., Husby, T. G. and Botzen, W. J. W.: Combining hazard, exposure and social vulnerability to provide lessons for flood risk management, Environ. Sci. Policy, 47, 42–52, doi:10.1016/j.envsci.2014.10.013, 2015.

Komolafe, A. A., Herath, S. and Avtar, R.: Development of generalized loss functions for rapid estimation of flood damages: a case study in Kelani River basin, Sri Lanka, Appl. Geomatics, 10(1), 13–30, doi:10.1007/s12518-017-0200-4, 2018.

Li, K., Wu, S., Dai, E. and Xu, Z.: Flood loss analysis and quantitative risk assessment in China, Nat. Hazards, 63(2), 737–760, doi:10.1007/s11069-012-0180-y, 2012.

Li, N., Zhang, Z., Chen, X. and Feng, J.: Importance of economic loss evaluation in natural hazard and disaster research, Prog. Geogr., 36(2), 256–263, doi:10.18306/dlkxjz.2017.02.011, 2017.

Limpert, E., Stahel, W. A. and Abbt, M.: Log-normal distributions across the sciences: Keys and clues, Bioscience, 51(5), 341–352, doi:10.1641/0006-3568(2001)051[0341:LNDATS]2.0.CO;2, 2001.

Merz, B., Kreibich, H., Thieken, A. and Schmidtke, R.: Estimation uncertainty of direct monetary flood damage to buildings, Nat. Hazards Earth Syst. Sci., 4(1), 153–163, doi:10.5194/nhess-4-153-2004, 2004.

Merz, B., Kreibich, H., Schwarze, R. and Thieken, A.: Review article "assessment of economic flood damage," Nat. Hazards Earth Syst. Sci., 10(8), 1697–1724, doi:10.5194/nhess-10-1697-2010, 2010.

Ministry of Housing and Urban-Rural Development (MHURD): Code for classification of urban land use and planning standards of development land, China., 2011.

Ministry of Housing and Urban-Rural Development (MHURD): Technical guide for sponge cities-water system construction of low impact development. [online] Available from: http://jst.jl.gov.cn/csjs/wjxx/201412/P020141222565834965487.pdf, 2014.

Mo, W. and Fang, W.: Empirical vulnerability functions of building contents to flood based on post-typhoon (Fitow, 201323) questionnaire survey in Yuyao, Zhejiang, Trop. Geogr., 36(4), 633-641+657, doi:https://doi.org/10.13284/j.cnki.rddl.002828, 2016.

NRC: Canadian guidelines and database of flood vulnerability functions, Canada, Natural Resources Canada, Public Safety Canada., 2017.

Penning-Rowsell, E. C., Yanyan, W., Watkinson, A. R., Jiang, J. and Thorne, C.: Socioeconomic scenarios and flood damage assessment methodologies for the Taihu Basin, China, J. Flood Risk Manag., 6(1), 23–32, doi:10.1111/j.1753-318X.2012.01168.x, 2013.

Pinelli, J. P., Da Cruz, J., Gurley, K., Paleo-Torres, A. S., Baradaranshoraka, M., Cocke, S. and Shin, D.: Uncertainty reduction through data management in the development, validation, calibration, and operation of a hurricane vulnerability model, Int. J. Disaster Risk Sci., 11(6), 790–806, doi:10.1007/s13753-020-00316-4, 2020.

Qie, Z. and Rong, L.: An integrated relative risk assessment model for urban disaster loss in view of disaster system theory, Nat. Hazards, 88(1), 165–190, doi:10.1007/s11069-017-2861-z, 2017.

~~Reese, S. and Ramsay, D.: RiskScape: Flood fragility methodology, Wellington: New Zealand Climate Change Research Institute., 2010.~~

Scawthorn, C., Asce, F., Flores, P., Blais, N., Seligson, H., Tate, E., Chang, S., Mifflin, E., Thomas, W., Murphy, J., Jones, C. and Lawrence, M.: HAZUS-MH Flood Loss Estimation Methodology. II. Damage and Loss Assessment, Nat. Hazards Rev., 7(2), 72–81, doi:10.1061/ASCE1527-6988200667:272, 2006.

Shen, Y., Zhao, P., Pan, Y. and Yu, J.: A high spatiotemporal gauge-satellite merged precipitation analysis over China, J. Geophys. Res. Atmos., 119, 3063–3075, doi:https://doi.org/10.1002/2013JD020686, 2014.

Shi, Y.: Research on vulnerability assessment of cities on the disaster scenario: A case study of Shanghai city, East China Normal University, Shanghai, China., 2010.

~~Smith D: Flood damage estimation A review of urban stage damage curves and loss functions, Water SA, 20(3), 231–238, 1994.~~

Stephenson, V. and D'Ayala, D.: A new approach to flood loss estimation and vulnerability assessment for historic buildings in England, Nat. Hazards Earth Syst. Sci. Discuss., 1(5), 6025–6060, doi:10.5194/nhessd-1-6025-2013, 2013.

UNISDR: The Pocket GAR 2015 Making Development Sustainable: The Future of Disaster Risk Management, Geneva, Switzerland: United Nations Office for Disaster Risk Reduction (UNISDR)., 2015.

USACE (United States Army Corps of Engineers): Depth-damage relationships for structures, contents, and vehicles and content-to-structure value ratios (CSVR) in support of the Donaldsonville to the Gulf, Louisiana, feasibility study, New Orleans District, Louisiana., 2006.

Wehner, M., Canterford, S., Corby, N., Edwards, M. and Juskevics, V.: Vulnerability of Australian houses to riverine inundation: analytical and empirical vulnerability curves, Canberra: Geoscience Australia., 2017.

Yu, K., Li, D., Yuan, H., Fu, W., Qiao, Q. and Wang, S.: "Sponge City": theory and practice, City Plan. Rev., 39(6), 26–36, doi:10.11819/cpr20150605a, 2015.

Zhao, Y., Gong, Z., Wang, W. and Luo, K.: The comprehensive risk evaluation on rainstorm and flood disaster losses in China mainland from 2004 to 2009: Based on the triangular gray correlation theory, Nat. Hazards, 71(2), 1001–1016, doi:10.1007/s11069-013-0698-7, 2014.

Zhou, Y., Lu, G., Jin, J., Tong, F. and Zhou, P.: A high precision comprehensive evaluation method for flood disaster loss based on improved genetic programming, J. Ocean Univ. China, 5(4), 322–326, doi:10.1007/s11802-006-0023-0, 2006.